https://ntrs.nasa.gov/search.jsp?R=19930091916 2020-06-17T03:31:15+00:00Z

NATIONAL ADVISORY COMMITTEE FOR AERONAUTICS

REPORT No. 840

STALLING OF HELICOPTER BLADES

By F. B. GUSTAFSON and G. C. MYERS, Jr.

CASE FILE COPY

1946

For sale by the Superintendent of Documents, U. S. Government Printing Office, Washington 25, D. C. - - - - - Price 10 cents

AERONAUTIC SYMBOLS

1. FUNDAMENTAL AND DERIVED UNITS

	Symbol	Metric		English	
		Unit	Abbreviation	Unit	Abbreviation
Length	l	meter	m	foot (or mile)	ft (or mi)
Time	t	second	s	second (or hour)	sec (or hr)
Force	F	weight of 1 kilogram	kg	weight of 1 pound	lb
Power	P	horsepower (metric)		horsepower	hp
Speed	V	kilometers per hour	kph	miles per hour	mph
		meters per second	mps	feet per second	fps

2. GENERAL SYMBOLS

W Weight$=mg$

g Standard acceleration of gravity$=9.80665$ m/s^2 or 32.1740 ft/sec^2

m Mass$=\frac{W}{g}$

I Moment of inertia$=mk^2$. (Indicate axis of radius of gyration k by proper subscript.)

μ Coefficient of viscosity

ν Kinematic viscosity

ρ Density (mass per unit volume)

Standard density of dry air, 0.12497 kg-m^{-4}-s^2 at 15° C and 760 mm; or 0.002378 lb-ft^{-4} sec^2

Specific weight of "standard" air, 1.2255 kg/m^3 or 0.07651 lb/cu ft

3. AERODYNAMIC SYMBOLS

S Area

S_w Area of wing

G Gap

b Span

c Chord

A Aspect ratio, $\frac{b^2}{S}$

V True air speed

q Dynamic pressure, $\frac{1}{2}\rho V^2$

L Lift, absolute coefficient $C_L=\frac{L}{qS}$

D Drag, absolute coefficient $C_D=\frac{D}{qS}$

D_0 Profile drag, absolute coefficient $C_{D_0}=\frac{D_0}{qS}$

D_i Induced drag, absolute coefficient $C_{D_i}=\frac{D_i}{qS}$

D_p Parasite drag, absolute coefficient $C_{D_p}=\frac{D_p}{qS}$

C Cross-wind force, absolute coefficient $C_C=\frac{C}{qS}$

i_w Angle of setting of wings (relative to thrust line)

i_t Angle of stabilizer setting (relative to thrust line)

Q Resultant moment

Ω Resultant angular velocity

R Reynolds number, $\rho\frac{Vl}{\mu}$ where l is a linear dimension (e.g., for an airfoil of 1.0 ft chord, 100 mph, standard pressure at 15° C, the corresponding Reynolds number is 935,400; or for an airfoil of 1.0 m chord, 100 mps, the corresponding Reynolds number is 6,865,000)

α Angle of attack

ϵ Angle of downwash

α_o Angle of attack, infinite aspect ratio

α_i Angle of attack, induced

α_a Angle of attack, absolute (measured from zero-lift position)

γ Flight-path angle

REPORT No. 840

STALLING OF HELICOPTER BLADES

By F. B. GUSTAFSON and G. C. MYERS, Jr.

Langley Memorial Aeronautical Laboratory
Langley Field, Va.

National Advisory Committee for Aeronautics

Headquarters, 1500 New Hampshire Avenue NW, Washington 25, D. C.

Created by act of Congress approved March 3, 1915, for the supervision and direction of the scientific study of the problems of flight (U. S. Code, title 49, sec. 241). Its membership was increased to 15 by act approved March 2, 1929. The members are appointed by the President, and serve as such without compensation.

JEROME C. HUNSAKER, Sc. D., Cambridge, Mass., *Chairman*

THEODORE P. WRIGHT, Sc. D., Administrator of Civil Aeronautics, Department of Commerce, *Vice Chairman.*

Hon. WILLIAM A. M. BURDEN, Assistant Secretary of Commerce.

VANNEVAR BUSH, Sc. D., Chairman, Joint Research and Development Board.

EDWARD U. CONDON, PH. D., Director, National Bureau of Standards.

R. M. HAZEN, B. S., Chief Engineer, Allison Division, General Motors Corp.

WILLIAM LITTLEWOOD, M. E., Vice President, Engineering, American Airlines System.

EDWARD M. POWERS, Major General, United States Army, Assistant Chief of Air Staff–4, Army Air Forces, War Department.

ARTHUR W. RADFORD, Vice Admiral, United States Navy, Deputy Chief of Naval Operations (Air), Navy Department.

ARTHUR E. RAYMOND, M. S., Vice President, Engineering, Douglas Aircraft Co.

FRANCIS W. REICHELDERFER, Sc. D., Chief, United States Weather Bureau.

LESLIE C. STEVENS, Rear Admiral, United States Navy, Bureau of Aeronautics, Navy Department.

CARL SPAATZ, General, United States Army, Commanding General, Army Air Forces, War Department.

ALEXANDER WETMORE, Sc. D., Secretary, Smithsonian Institution.

ORVILLE WRIGHT, Sc. D., Dayton, Ohio.

GEORGE W. LEWIS, Sc. D., *Director of Aeronautical Research*

JOHN F. VICTORY, LLM., Executive Secretary

HENRY J. E. REID, Sc. D., Engineer-in-charge, Langley Memorial Aeronautical Laboratory, Langley Field, Va.

SMITH J. DEFRANCE, B. S., Engineer-in-charge, Ames Aeronautical Laboratory, Moffett Field, Calif.

EDWARD R. SHARP, LL. B., Manager, Aircraft Engine Research Laboratory, Cleveland Airport, Cleveland, Ohio

CARLTON KEMPER, B. S., Executive Engineer, Aircraft Engine Research Laboratory, Cleveland Airport, Cleveland, Ohio

---

TECHNICAL COMMITTEES

AERODYANMICS
POWER PLANTS FOR AIRCRAFT
AIRCRAFT CONSTRUCTION
OPERATING PROBLEMS
MATERIALS RESEARCH COORDINATION
SELF-PROPELLED GUIDED MISSILES
SURPLUS AIRCRAFT RESEARCH
INDUSTRY CONSULTING COMMITTEE

Coordination of Research Needs of Military and Civil Aviation
Preparation of Research Programs
Allocation of Problems
Prevention of Duplication
Consideration of Inventions

LANGLEY MEMORIAL AERONAUTICAL LABORATORY, Langley Field, Va.

AMES AERONAUTICAL LABORATORY, Moffett Field, Calif.

AIRCRAFT ENGINE RESEARCH LABORATORY, Cleveland Airport, Cleveland, Ohio

Conduct, under unified control, for all agencies, of scientific research on the fundamental problems of flight

---

OFFICE OF AERONAUTICAL INTELLIGENCE, Washington, D. C.

Collection, classification, compilation, and dissemination of scientific and technical information on aeronautics

REPORT No. 840

STALLING OF HELICOPTER BLADES

By F. B. Gustafson and G. C. Myers, Jr.

SUMMARY

Theoretical studies have predicted that operation of a helicopter rotor beyond certain combinations of thrust, forward speed, and rotational speed might be prevented by rapidly increasing stalling of the retreating blade. The same studies also indicate that the efficiency of the rotor will increase until these limits are reached or closely approached, so that it is desirable to design helicopter rotors for operation close to the limits imposed by blade stalling. Inasmuch as the theoretical predictions of blade stalling involve numerous approximations and assumptions, an experimental investigation was needed to determine whether, in actual practice, the stall did occur and spread as predicted and to establish the amount of stalling that could be present without severe vibration or control difficulties being introduced.

The results of such an investigation of a typical helicopter are presented herein. Photographic observations of tufts on the rotor blades show that, for the rotor studied, the stall did occur and spread roughly in the manner predicted. Correlation of the tuft photographs with pilot's observations of vibration and control characteristics show that the effects of stalling on stick vibration and control are severe for this helicopter when the calculated angle of attack at the tip of the retreating blade exceeds the stalling angle of the airfoil section by approximately 4°.

Theoretical design charts, constructed on the assumption that tip angles of attack cannot be permitted to exceed the stall by more than 4°, show how blade stalling in combination with compressibility effects may be expected to hamper the designer in his efforts to develop high-speed helicopters. These charts also indicate some of the means by which stalling limits may be postponed and the magnitude of the gains that might be achieved.

Blade stalling is concluded to be an important obstacle in the development of high-speed helicopters, and the investigation of the various known methods of delaying blade stall may make possible substantial speed increases.

INTRODUCTION

As a lifting rotor moves forward, the advancing blades encounter progressively higher velocities and the retreating blades, progressively lower velocities. Thus, in order to maintain its lift, the retreating blade must operate at progressively higher angles of attack as forward speed is increased. It follows that at some ratio of forward speed to rotational speed the angles of attack on the retreating blade will reach the stall.

Theoretical analyses presented in references 1 and 2 show that the best rotor efficiency in forward flight is obtained by operating at tip speeds at which stalling begins to become significant. The analysis of reference 3 has shown that, if this procedure is not followed, a sacrifice in hovering efficiency will result. Conflicting with these considerations of efficiency are practical considerations of safety and freedom from vibration, inasmuch as designing the rotor for the condition where stall becomes significant leaves no margin for maneuvers or gusts, and the pilot, when encountering these conditions, would find the effects of stall extremely serious. The net result is that blade stall is a highly significant criterion of design and, in the final analysis, determines the ultimate possibilities of the helicopter.

A great deal of work has previously been done on rotors operating in the autorotative condition. These studies have indicated that stalling of the blades did occur in flight roughly in the manner expected from rotor theory; that is, in the case of the autogiro, the stall was found to occur first inboard on the retreating blade in the low-velocity region, then to spread outward, and eventually to approach the higher velocities near the tip. The stalled region should be quite different for the helicopter than for the autogiro, owing to the reversal of direction of inflow. An experimental study was therefore made on a helicopter rotor for correlation with the corresponding theory.

SYMBOLS

μ tip-speed ratio $\left(\frac{V\cos\alpha}{\Omega R}\right)$

V true airspeed, feet per second except where otherwise noted

Ω rotor angular velocity, radians per second

R rotor blade radius, feet

α angle of attack of rotor disk, degrees

C_T thrust coefficient $\left(\frac{T}{\rho(\Omega R)^2\pi R^2}\right)$

T thrust, pounds

ρ air density, slugs per cubic foot

σ solidity $\left(\frac{bc_e}{\pi R}\right)$

b number of blades

c_e equivalent chord $\left(\frac{\int_0^R cr^2dr}{\int_0^R r^2dr}\right)$

c blade chord, feet

r radius to blade element, feet

α_r angle of attack of blade element, degrees

ψ blade azimuth angle measured from down-wind position in direction of rotation

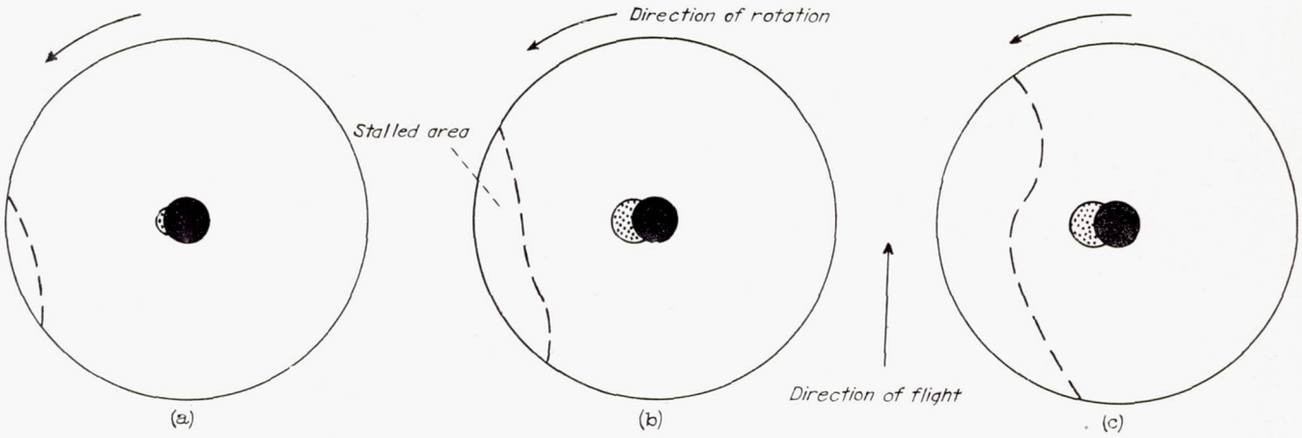

(a) V=40 mph; rotor speed, 205 pm. (μ=0.153; $\frac{C_T}{\sigma}$=0.109.)

(b) V=70 mph; rotor speed, 225 rpm. (μ=0.230; $\frac{C_T}{\sigma}$=0.091.)

(c) V=70 mph; rotor speed, 205 rpm. (μ=0.249; $\frac{C_T}{\sigma}$=0.105.)

FIGURE 1.—Theoretical stall boundaries for representative helicopter conditions. Weight 2580 pounds; radius, 19 feet; parasite-drag area, 23 square feet; stalling angle of attack, 12°.

THEORETICAL ANALYSIS

If the angle-of-attack distribution around the rotor is calculated for some representative conditions of flight, it is possible to see where the stalled region is expected on the helicopter rotor and how large it may become. Results of calculations for representative flight conditions are shown in figure 1. The values of airspeed and rotor speed used to identify the three conditions illustrated in figure 1 are somewhat approximate, the values used in the calculations having been chosen to correspond to specific flight data which will be discussed subsequently. The circles shown in the figure represent plan views of the rotor disk, the direction of flight and direction of rotation being as shown. The dark region at the center represents the area swept by the hub and blade shanks. The shaded crescents represent the region where the direction of flow over the retreating blades is reversed. Wind-tunnel tests on practical-construction sections of the blades used indicate that the stalling angle is about 12°. Consequently, the contour for an angle of attack of 12° has been drawn and is considered as the boundary of the stalled region. All angles of attack inboard of this boundary are less than 12°. Angles outboard are greater than 12° and this region is considered stalled.

For the helicopter under consideration, it would be expected on the basis of the calculations that stalling would be just beginning to occur on the retreating tip at a forward speed of 40 miles per hour and a rotor speed of 205 rpm (fig. 1 (a)). Similarly, at a forward speed of 70 miles per hour and a rotor speed of 225 rpm an increased region of stall is expected (fig. 1 (b)), and at low rotor speed and a forward speed of 70 miles per hour (fig. 1 (c)) an appreciable stalled area would be anticipated.

These calculations are based upon reference 4, which makes certain simplifying assumptions and takes no account of the effect of the stall itself on the blade motion and thus the angle-of-attack distribution.

EXPERIMENTAL METHOD

In order to obtain experimental data for the present investigation, the type of equipment described in reference 5 was used. A 35-millimeter motion-picture camera was mounted rigidly on the rotor hub and was pointed along a blade equipped with tufts and markings. (See fig. 2.) The tufts were pieces of wool yarn 3 inches long. In figure 3 typical photographs from the records taken in flight are shown. In figure 3 (a) the blade is on the advancing side. Note that all the tufts indicate smooth flow along the blade. In figure 3 (b), which is a photograph taken on the retreating side, it can be seen that the outer portion of the blade is definitely stalled, the tufts streaming forward from their attachment points. Similarly, the blade at the 0.75 radius is stalled, at the 0.6 radius is partly stalled, and at the 0.45 radius is unstalled though the flow is heavily yawed. The

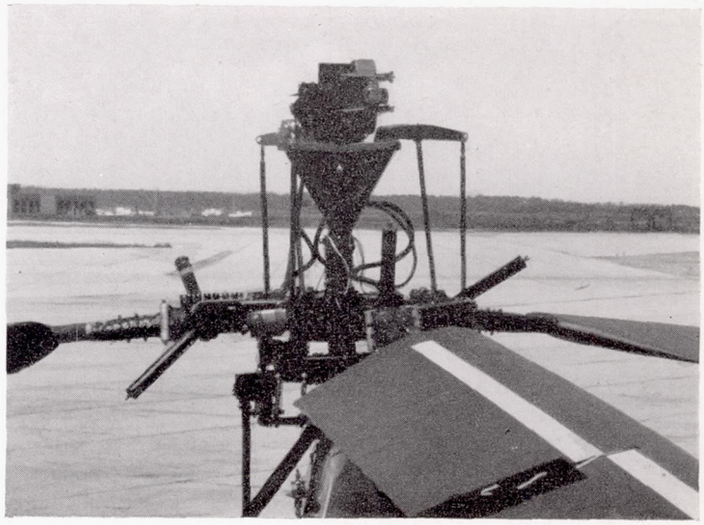

FIGURE 2.—Camera installation on helicopter rotor hub.

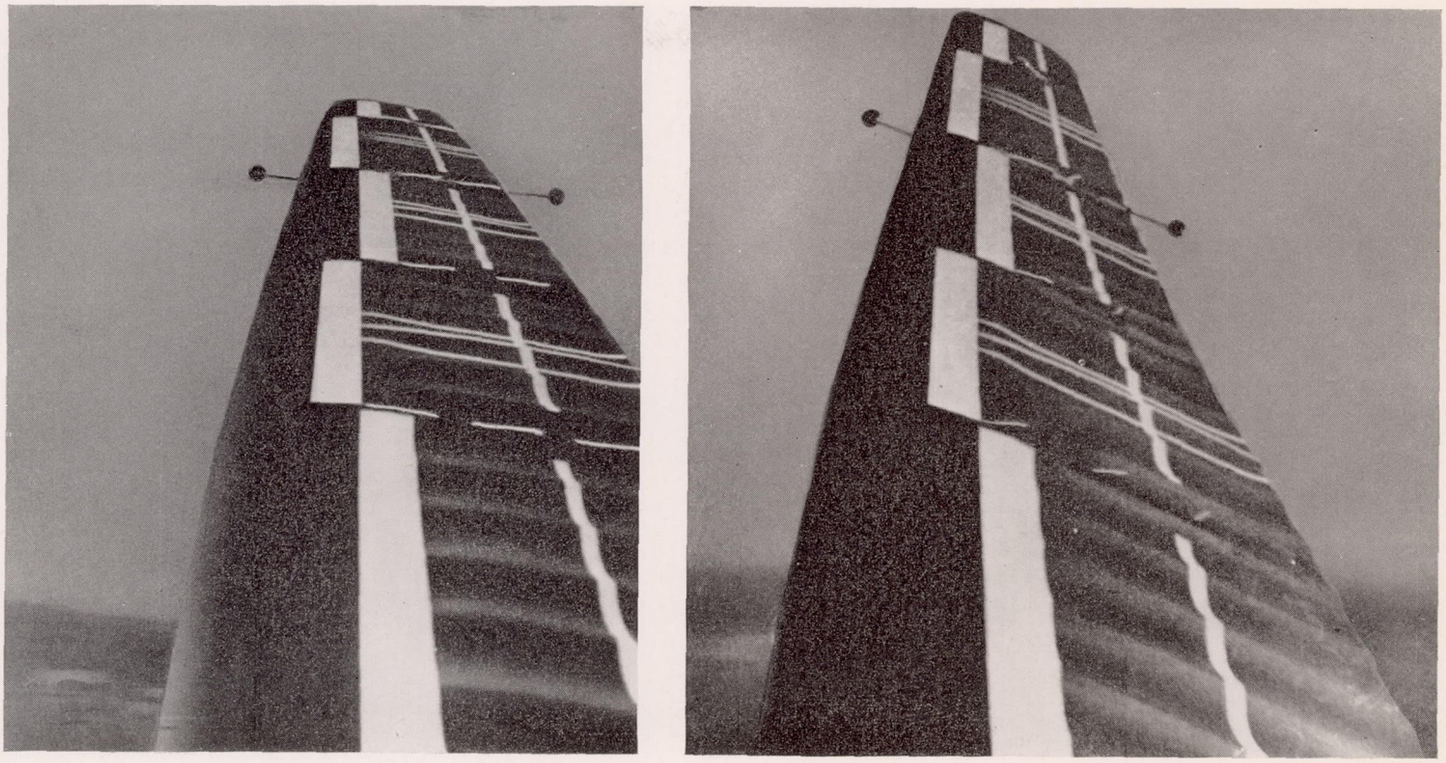

(a) $\psi=70°$. (b) $\psi=310°$.

FIGURE 3.—Typical photographs taken in flight of tufts on a helicopter rotor blade.

blade section was considered to be stalled when the tufts indicated reversed or burbled flow over the rear 30 percent of the chord.

RESULTS AND DISCUSSION

Some of the results obtained from analyzing the photographs of the blades, such as figure 3, are shown in figure 4. The observed stall regions, represented by the shaded areas, have been superimposed upon the theoretically established regions for the same conditions shown in figure 1. It is seen that the stall does occur and grow roughly in the expected manner.

Pilot reactions to the conditions are quite interesting. The condition at a forward speed of 70 miles per hour and low rotor speed (fig. 4 (c)) where a large amount of stalling is present represents the most extreme condition that the pilot was able to maintain long enough to take a record.

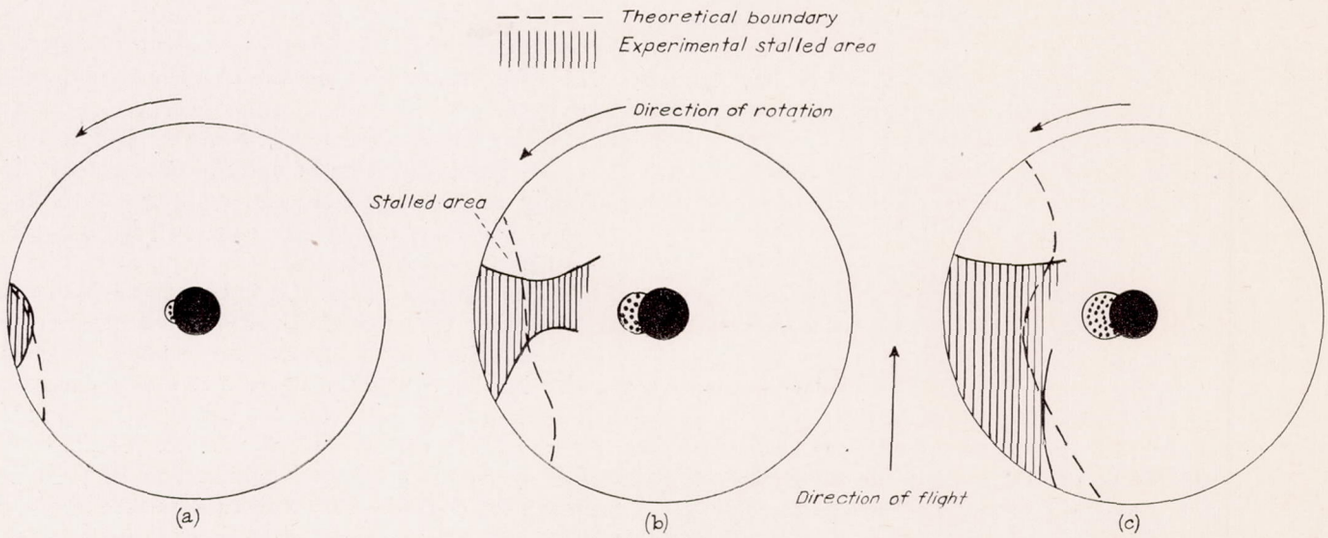

(a) $V=40$ mph; rotor speed, 205 rpm. (b) $V=70$ mph; rotor speed, 225 rpm. (c) $V=70$ mph; rotor speed, 205 rpm.

FIGURE 4.—Comparison between theoretical and experimental stalled areas.

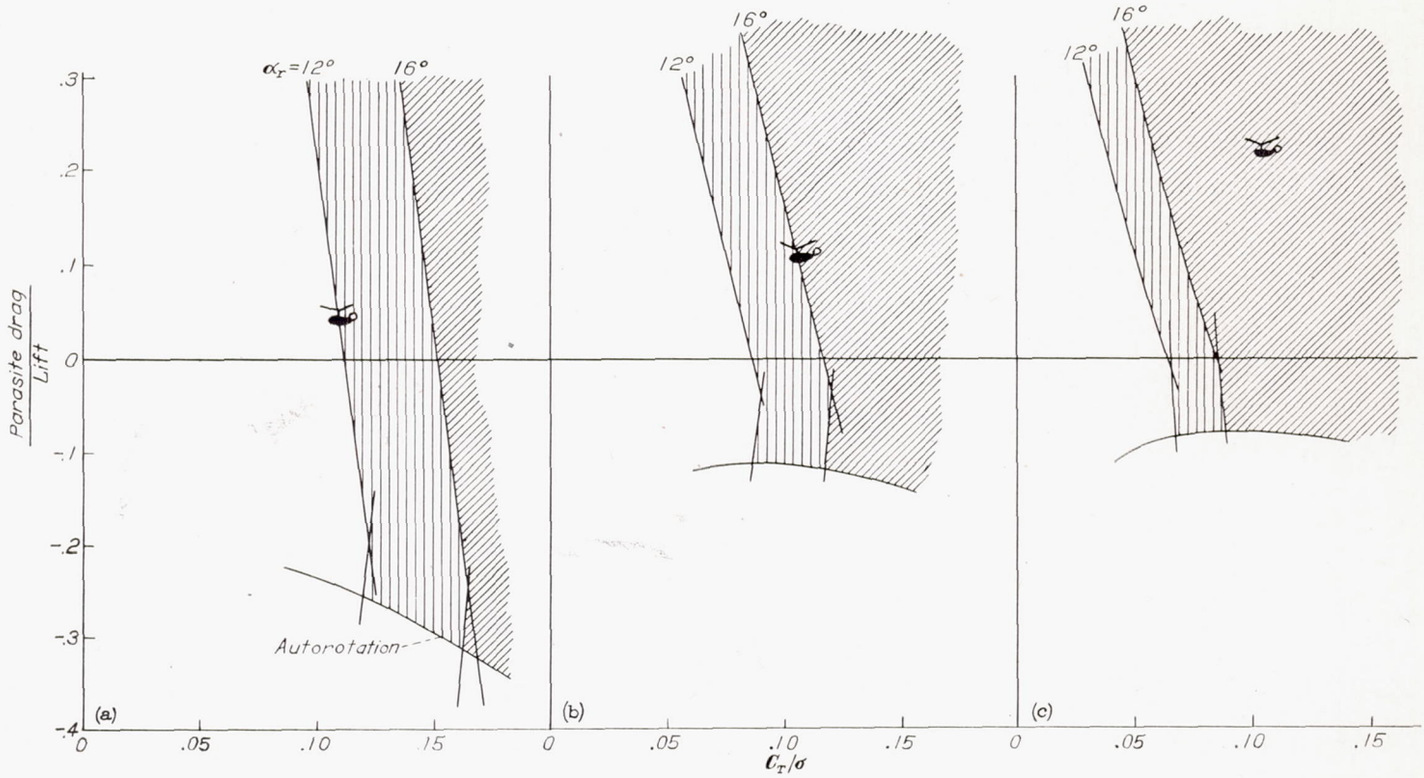

(a) μ=0.15. (b) μ=0.25. (c) μ=0.35.

FIGURE 5.—Theoretical stalling-angle plots.

For this helicopter, therefore, the condition with this large stalled area (about 15 percent of the disk area) appears to represent very nearly the operational limit.

In the condition of moderate stall, the pilot although uncomfortable was able to control the helicopter satisfactorily and to take records. No effects that would be associated with stalling were noted in the first marginal stall case. It would seem then that, although the effects of a small amount of stalling are tolerable, operation with large amounts of stall is prohibitive.

From the preceding discussion stalling would be expected to impose a real limit on the condition of operation that may be utilized. It is interesting to examine the possibility of correlating practical experience with rotor theory in this regard and also to examine the influence of the design variables on the theoretical stalling limits. A convenient plot for such examination is shown in figure 5.

The angle of attack reached at the retreating tip of the blade depends upon the three variables shown in figure 5. It depends first upon the tip-speed ratio μ, that is, the ratio of forward speed to rotational speed. It also depends upon the ratio of the thrust coefficient to the solidity C_T/σ (which is a measure of the mean blade lift coefficient) for, as the angles of attack all around the disk increase, the angle of the retreating tip also increases. For a given helicopter, this quantity C_T/σ may be increased either by increasing the weight or by decreasing the rotational speed. It will also be increased by operation at high altitudes. For efficient operation this mean lift coefficient should be kept reasonably high. Finally, the angle of attack at the retreating tip depends upon the ratio of parasite drag to lift; that is, the degree to which the thrust vector must tilt forward to overcome the drag of the fuselage. If a propeller is installed on the fuselage, it is possible, in effect, to reduce the parasite drag which the rotor must overcome. In fact, with increased propeller power, negative values of parasite drag can be produced. Then, although for positive values of parasite drag the rotor is dragging the fuselage, for negative values the propeller and fuselage are dragging the rotor and the limiting condition is that of the autogiro, for which no power is being applied to the rotor. Thus, increasing the ratio of parasite drag to lift (fig. 5) is equivalent to applying more and more power to the rotor. Values of the ratio of parasite drag to lift for present-day helicopters at cruising speeds are of the order of 0.1.

Once the tip-speed ratio μ is fixed, the angle of attack at the retreating tip is determined for combinations of the ratio of parasite drag to lift and mean blade lift coefficient. The line labeled $\alpha_r=12°$ in figure 5 represents combinations of these quantities for which the calculated angle of attack at the retreating tip (at $\psi=270°$) is 12°. Similarly, the line labeled $\alpha_r=16°$ represents combinations of parasite drag and mean lift coefficient for which the retreating tip angle of attack is 16°. Because the stall begins inboard in the autorotation or near-autorotation conditions, the type of inboard limit adopted in reference 2 has been used for conditions

where this limit is more stringent than the tip angle-of-attack limitation. The condition represented by the short limit lines touching the curves labeled "autorotation" in figure 5 is that the blade angle of attack shown has been reached at 270° azimuth at a radius such that the tangential velocity is equal to four-tenths the rotational tip speed. The 12° and 16° lines represent the range of angle of attack in which blade airfoils would be expected to stall and have been included in previous theoretical papers as probable limiting conditions of the validity of the theory.

The positions of the curves on figure 5 show, then, that increasing either C_T/σ, the ratio of parasite drag to lift, or μ increases the angle of attack at the retreating tip.

Now that these theoretical relationships have been established, it is of interest to spot selected data points on the plots. The condition for which extreme stall was observed in flight was at a forward speed of 70 miles per hour and a rotor speed of 205 rpm, which corresponds to a tip-speed ratio μ of approximately 0.25. This condition applies therefore to the plot of figure 5 (b). For this condition the values of the ratio of parasite drag to lift and C_T/σ locate the point as shown. Since this point represents the extreme amount of tip stall operationally tolerable, it would appear that, for this rotor, the 16° tip angle-of-attack line may be taken as the limit of practical conditions of operation. If in a similar manner the point at which stall was just beginning to occur is plotted (for a forward speed of 40 mph and a rotor rotational speed of 205 rpm, giving a tip-speed ratio of approx. 0.15 and locating the point on the plot of figure 5 (a)), it is found that the coordinate values are such as to place the point on the 12° angle-of-attack line. This result indicates again the agreement with theory shown earlier for this marginal stall case. It will be noted that, for the helicopter tested, the operational limit occurred when the calculated angle of attack at the tip of the retreating blade exceeded the stalling angle of the airfoil section by approximately 4°. The 12° and 16° angle-of-attack lines may be considered boundaries of three regions, the first representing conditions for which no stall will be encountered, the second (hatched region in fig. 5) representing conditions for which a moderate amount of stall is present, and the third (cross-hatched region in fig. 5) representing conditions for which stall is so severe as to prohibit operation.

If, for example, an attempt were made to fly this helicopter at 100 miles per hour, and hence at a tip-speed ratio of approximately 0.35, and still use the low rotor speed used in the first two cases, the operating condition would be far beyond the 16° angle-of-attack line that represents the maximum tolerable amount of stall. This point is shown in figure 5 (c).

The combinations of these variables which the designer may use are limited by the necessity for working in the operationally feasible region. As the tip-speed ratio is increased, the region of possible operating conditions grows smaller and smaller until, finally, at some higher tip-speed ratio, the area free from stall disappears entirely. The permissible blade loading C_T/σ approaches zero and, thus, the load that can be carried also approaches zero. The tip-speed ratio which may be attained is therefore limited by stalling. If large increases in the high speed of the helicopter are attempted, accompanying increases in the rotational speed must, of necessity, be made in order to keep down the tip-speed ratio and avoid severe stalling. Large increases in rotational speed, however, lead to compressibility losses at the blade tips. The degree to which low tip-speed ratios can be maintained with increasing forward speed is therefore limited by compressibility. Tip stall and compressibility thus ultimately limit the high speed of the helicopter.

The higher the loadings that the designer attempts to maintain, the lower are the tip-speed ratios which can be attained without severe stalling; and the lower the permissible tip-speed ratios, the lower is the forward speed at which compressibility troubles occur. High loadings thus involve low limiting speeds and, conversely, high speeds necessitate low loadings. The high-speed helicopter must therefore be lightly loaded, which suggests a large rotor of high solidity operating at high tip speeds.

Figure 5 also indicates a number of ways in which the helicopter designer may postpone the stall without incurring penalties in performance elsewhere. Very significant gains are available if the stalling characteristics of present-day rotor blades are improved. Two means are available for increasing the stalling angle: (1) irregularities in the section that induce premature stall should be avoided and (2) airfoil profiles having higher stalling angles may be used insofar as is possible without producing drag increases at low angles and without producing large pitching moments. Another possibility from which only benefits accrue is cleaning up the fuselage, since reducing the parasite drag has already been shown to reduce the angle of attack in the region of the stall.

A reduction in C_T/σ or in the mean blade lift coefficient is undesirable because of penalties incurred elsewhere, for example, in hovering and cruising flight. One way to avoid this problem, however, is by the use of a gear shift. The helicopter may be designed for high speed on the basis of compressibility and stall limits (which factors call for use of a low mean lift coefficient) and a gear shift may be provided to permit reduction of the rotor rotational speed in hovering and in low-speed operation. The mean lift coefficients may thus be raised to efficient values for these conditions.

It may also be remarked that the introduction of some twist in the blades shows promise of delaying the stall, since it tends to distribute the lift more evenly along the blades and to reduce the high loadings at the tip.

CONCLUSIONS

On the basis of the limited experimental and theoretical treatments presented, the following conclusions concerning the stalling of helicopter blades may be drawn:

1. Stall occurs and spreads roughly in the manner predicted by helicopter theory.

2. Stalling imposes a practical limit on the condition of operation which may be utilized. For the helicopter tested,

the operational limit occurred when the angle of attack at the tip of the retreating blade exceeded the stalling angle of the airfoil by approximately 4°.

3. The extent of the experimental data and the degree of agreement shown are believed to be sufficient to indicate that theoretical stalling calculations can be used as a basis for helicopter rotor design.

4. Further correlation of data with theory and study of the avenues open for postponing the stall should be extremely helpful in realizing the ultimate possibilities of the helicopter.

Langley Memorial Aeronautical Laboratory,
National Advisory Committee for Aeronautics,
Langley Field, Va., *April 15, 1946*.

REFERENCES

1. Gustafson, F. B.: Effect on Helicopter Performance of Modifications in Profile-Drag Characteristics of Rotor-Blade Airfoil Sections. NACA ACR No. L4H05, 1944.
2. Bailey, F. J., Jr., and Gustafson, F. B.: Charts for Estimation of the Characteristics of a Helicopter Rotor in Forward Flight. I—Profile Drag-Lift Ratio for Untwisted Rectangular Blades. NACA ACR No. L4H07, 1944.
3. Gustafson. F. B., and Gessow, Alfred: Effect of Rotor-Tip Speed on Helicopter Hovering Performance and Maximum Forward Speed. NACA ARR No. L6A16, 1946.
4. Bailey, F. J., Jr.: A Simplified Theoretical Method of Determining the Characteristics of a Lifting Rotor in Forward Flight. NACA Rep. No. 716, 1941.
5. Bailey, F. J., Jr., and Gustafson, F. B.: Observations in Flight of the Region of Stalled Flow over the Blades of an Autogiro Rotor. NACA TN No. 741, 1939.

U. S. GOVERNMENT PRINTING OFFICE: 1948

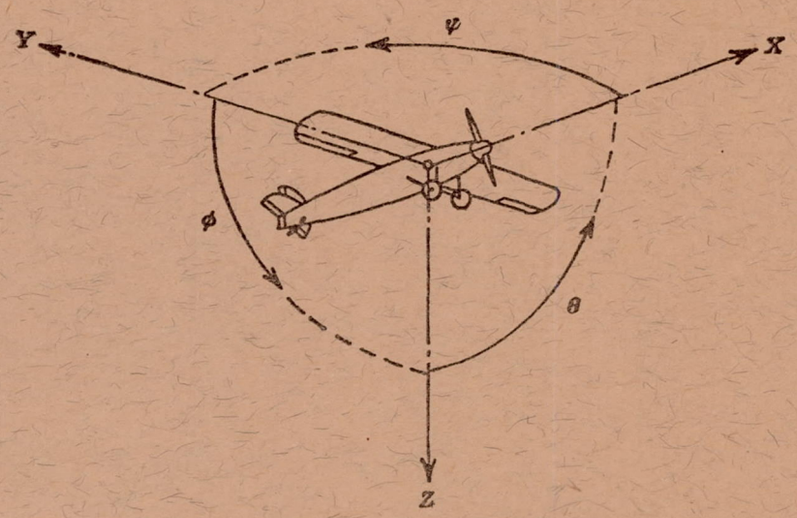

Positive directions of axes and angles (forces and moments) are shown by arrows

Axis		Force (parallel to axis) symbol	Moment about axis			Angle		Velocities	
Designation	Symbol		Designation	Symbol	Positive direction	Designation	Symbol	Linear (component along axis)	Angular
Longitudinal	X	X	Rolling	L	$Y \longrightarrow Z$	Roll	φ	u	p
Lateral	Y	Y	Pitching	M	$Z \longrightarrow X$	Pitch	θ	v	q
Normal	Z	Z	Yawing	N	$X \longrightarrow Y$	Yaw	ψ	w	r

Absolute coefficients of moment

$C_l=\frac{L}{qbS}$ (rolling) $\quad C_m=\frac{M}{qcS}$ (pitching) $\quad C_n=\frac{N}{qbS}$ (yawing)

Angle of set of control surface (relative to neutral position), δ. (Indicate surface by proper subscript.)

4. PROPELLER SYMBOLS

D Diameter

p Geometric pitch

p/D Pitch ratio

V' Inflow velocity

V_s Slipstream velocity

T Thrust, absolute coefficient $C_T=\frac{T}{\rho n^2 D^4}$

Q Torque, absolute coefficient $C_Q=\frac{Q}{\rho n^2 D^5}$

P Power, absolute coefficient $C_P=\frac{P}{\rho n^3 D^5}$

C_s Speed-power coefficient $=\sqrt[5]{\frac{\rho V^5}{P n^2}}$

η Efficiency

n Revolutions per second, rps

Φ Effective helix angle $=\tan^{-1}\left(\frac{V}{2\pi r n}\right)$

5. NUMERICAL RELATIONS

1 hp=76.04 kg-m/s=550 ft-lb/sec

1 metric horsepower=0.9863 hp

1 mph=0.4470 mps

1 mps=2.2369 mph

1 lb=0.4536 kg

1 kg=2.2046 lb

1 mi=1,609.35 m=5,280 ft

1 m=3.2808 ft